


Article

Transparent Celadon with Phase-Separated Structure: Study on the Technological Characteristics and Coloring Mechanism of Celadons from the Lieshan Kiln

Qijiang Li ^{1,2}, Jingyun Wang ¹, Chao Chen ^{2,3}, Tao Fang ^{1,2}, Chenyi Gao ¹ and Jinwei Li ^{1,2,*} ¹ Research Center of Ancient Ceramic, Jingdezhen Ceramic University, Jingdezhen 333001, China² Jiangxi Ceramic Heritage Conservation and Imperial Kiln Research Collaborative Innovation Center, Jingdezhen 333001, China³ Anhui Provincial Institute of Cultural Relics and Archaeology, Hefei 230601, China

* Correspondence: lijinwei@jcu.edu.cn

Abstract: The excavation of the Lieshan Kiln site represents a significant advance in the field of ceramic archaeology. Previous scholars fixated on the white porcelain unearthed from this kiln, yet this study zeroed in on celadon from the Northern Song and Jin Dynasties. Celadon samples were analyzed using colorimetry, energy-dispersive X-ray fluorescence spectroscopy (ED-XRF), scanning electron microscopy (SEM), polarizing microscopy, X-ray photoelectron spectroscopy (XPS), and thermal expansion analysis. Results revealed that material and technological advancements in the production of the Lieshan Kiln and reveal the special phase-separated structure in the glaze of the transparent celadon, with a weakly reduced firing atmosphere. Celadon bodies from both periods were crafted from local sedimentary clays in a single-ingredient formula, with the Jin Dynasty refining the preparation, leading to enhanced density and higher firing temperatures compared to the Northern Song Dynasty. The celadon glaze, a high-calcium type made up of glaze ash and specific clays, differed from the body materials. The high SiO₂/Al₂O₃ molar ratio, along with Fe₂O₃ and trace P₂O₅, promoted phase separation. Glaze coloration was modulated by the interaction of Fe³⁺ and Fe²⁺ ions, and chemical coloration by Fe ions prevailed when phase-separated particles were minute enough to avoid Rayleigh or Mie scattering. In conclusion, the study deepens the understanding of ancient ceramic production by exploring the phase separation structure and coloring mechanism of the celadon.

Keywords: Lieshan Kiln; celadon; phase-separated structure; coloring mechanism; chemical composition



check for updates

Academic Editor: Maria Gazda

Received: 23 December 2024

Revised: 13 January 2025

Accepted: 17 January 2025

Published: 20 January 2025

Citation: Li, Q.; Wang, J.; Chen, C.;

Fang, T.; Gao, C.; Li, J. Transparent

Celadon with Phase-Separated

Structure: Study on the Technological

Characteristics and Coloring

Mechanism of Celadons from the

Lieshan Kiln. *Crystals* **2025**, *15*, 95.[https://doi.org/10.3390/](https://doi.org/10.3390/cryst15010095)[cryst15010095](https://doi.org/10.3390/cryst15010095)**Copyright:** © 2025 by the authors.

Licensee MDPI, Basel, Switzerland.

This article is an open access article

distributed under the terms and

conditions of the Creative Commons

Attribution (CC BY) license

[\(https://creativecommons.org/](https://creativecommons.org/licenses/by/4.0/)[licenses/by/4.0/\).](https://creativecommons.org/licenses/by/4.0/)

1. Introduction

The Lieshan Kiln site has undergone two extensive archaeological excavations and studies between 2017 and 2018. This demonstrated its important role in the transmission of northern white porcelain to southern regions, thereby establishing its considerable historical significance [1]. The Lieshan kiln site has unearthed a large number of artifacts from the late Tang Dynasty to the Jin and Yuan periods, including a considerable quantity of celadon and white porcelain. Previous scholars have focused on white porcelain and conducted scientific analyses on the white porcelain specimens unearthed at the Lieshan Kiln, comparing them with those from northern kilns to prove that the Lieshan Kiln was greatly influenced by the northern kiln industry [2–4]. However, there are few studies on unearthed celadon. Ancient Chinese celadon has a long and storied history in its development and has attracted

considerable interest from researchers in the world. From the primitive celadon of the Shang and Zhou Dynasties to the emergence of southern celadon during the Han and Jin Dynasties, the continuous exchanges and advances in celadon production technology led to the development of distinctive characteristics of northern and southern celadon [5]. Among them, celadons from the Yue Kiln, Yaozhou Kiln, and Longquan Kiln are far and away the most famous. Previous studies have not only delved into the body, glaze color, and chemical composition of celadons from different regions to distinguish their characteristics but also extensively investigated the coloring mechanisms of celadons from different areas. It has been found that celadon from various regions differs not only in external features but also in microstructures and coloring mechanisms. For example, southern celadon is characterized by its hard and delicate body, a moist and jade-like glaze, and a soft luster [6–8]. In contrast, the northern variety is distinguished by a thick body, a strong glassy texture on the glaze, a high gloss, and fine crackling [9,10]. In the research on the Yue Kiln, Fe ions in the glaze exist either entirely in the form of Fe^{3+} or in the co-existence form of Fe^{2+} and Fe^{3+} . The coloring is closely related to the energy levels of iron [11,12]. The coloring of Yaozhou celadon is associated with its microstructure and the chemical color produced by iron elements, the high $\text{Fe}^{2+}/\text{Fe}^{3+}$ ratio, and the glassy phase separation droplet could well be linked to the color origin of sky-green celadon [13–17]. The colors of Longquan celadon vary in different periods, while its coloring primarily depends on the ratio of Fe^{3+} to Fe^{2+} [18,19]. Celadon glaze is a high-temperature transparent glaze with iron as the main coloring element. Its color is determined by the Fe content in the glaze and the valence and coordination state of the Fe ions, while the firing temperature, strength of the reducing atmosphere, and basic glaze acidity and alkalinity affect the valence and coordination state of the Fe ions [20,21]. Different contents of Fe_2O_3 can control the microstructure of the glaze melt, resulting in a phase-separated structure. This phase-separated structure has a decisive influence on celadon's color, glossiness, and overall artistic effect.

Here, celadon specimens from the Northern Song and Jin Dynasties provided by the Anhui Provincial Institute of Cultural Relics and Archaeology were selected as the target. In addition, we adopted an energy-dispersive X-ray fluorescence spectrometer (ED-XRF), scanning electron microscope (SEM), and thermal expansion tests to analyze the physical properties, the chemical composition of both body and glaze, the valence and coordination of the iron elements, and the microstructure. This comprehensive analysis aims to elucidate the coloring mechanisms and technological characteristics of the celadon unearthed from the the Lieshan Kiln. This study deepens our understanding of the development and characteristics of ancient ceramic preparation technology and provides substantial evidence for the advancement of kiln industry and porcelain-making techniques at the Lieshan Kiln. This holds significant implications for the historical study of ceramic development technologies.

2. Materials and Methods

2.1. Celadon Samples

Nine celadon specimens from the Northern Song Dynasty (BS1 to BS9) and eleven celadon specimens from the Jin Dynasty (JD1 to JD11) were selected in this study. All specimens were provided by the Anhui Provincial Institute of Cultural Relics and Archaeology based on stratigraphic nomenclature. These celadons are highly representative, with varying shades of color, and can comprehensively reflect the characteristics of the celadon produced by the Lieshan Kiln. The detailed characteristics of the samples are presented in Table S1. In order to facilitate the following tests, the celadon specimens were ultrasonically cleaned in deionized water for 30 min and then dried in an oven at $110\text{ }^\circ\text{C}$ for 2 h.

2.2. Characterization Techniques

A portable colorimeter NF-333 from Nippon Denshoku, Japan, was used to measure the chromaticity values of the glaze surface of the specimens. Specifically, the chromaticity measurements focused on obtaining color values ($L^*a^*b^*$). Here L^* indicates the brightness and a^* and b^* indicate color variation. The colorimeter was equipped with a multi-color LED light source with a beam diameter of 8 mm. Specimens were sectioned into rectangular prisms of 25 mm \times 5 mm \times 5 mm and their water absorption, apparent porosity, and bulk density were determined via the boiling water method. A DIL 402C dilatometer from Naichi, Germany, was used to analyze the firing temperature. The furnace temperature ranged from room temperature to 1300 °C with a heating rate of 10 K/min, and argon gas was used as the protective atmosphere. The specimens were cut into 5 mm \times 5 mm \times 5 mm cubes and their chemical composition at the body and glaze areas was tested using an Eagle III XXL ED-XRF (EDAX, Pleasanton, CA, USA). The tests were conducted under vacuum conditions with a beam diameter of 300 μ m, a voltage of 50 KV, a current of 200 μ A, and a test time of 200 s. A range of standard reference materials specifically designed for the non-destructive testing of ancient ceramics was used for these experiments. Standard curves were created for each element using the software Delta-1 supplied with the instrument. Some of the sectioned specimens were corroded with 5% hydrofluoric acid for 30 s and then ultrasonically cleaned in distilled water for 30 min after corrosion, dried, and gold-sputtered. The microstructure of the glaze surface was tested using a SU-8010 scanning electron microscope from Hitachi, Japan. A number of sectioned specimens were made into thin sections and observed for optical characteristics of the body and glaze using a ZEISS Axio Scope. A1 polarizing microscope from Carl Zeiss AG, Oberkochen, BW, Germany). Two specimens from different periods were cut into small cubes with a glazed surface of 5 mm \times 5 mm \times 2 mm and dried, and the relative content of Fe ions in different valence states was tested using an ESCALAB Xi+ X-ray photoelectron spectrometer from ThermoFisher, Waltham, MA, USA.

3. Results and Discussion

3.1. $L^*a^*b^*$ and Physical Properties

Color measurements of the specimens were made for L^* , a^* , and b^* values. The L^* value indicates brightness, ranging from 0 (black) to 100 (white), the a^* value represents the red–green spectrum, with negative values denoting green and positive values indicating red, while the b^* value reflects the yellow–blue spectrum, where negative values signify blue and positive values denote yellow. As presented in Table 1, the a^* values exhibit relative consistency, averaging approximately 0.9, which suggests a celadon hue. The b^* values were found to be positive, with averages of 20.81 for specimens from the Jin Dynasty and 11.12 for those from the Northern Song Dynasty. This indicates that the glaze during the Jin Dynasty was more yellowish-green compared to the Northern Song Dynasty. Furthermore, the higher the content of Fe_2O_3 and TiO_2 in the glaze, the deeper the glaze color, which is consistent with the observed appearance of the specimens. L^* , a^* , and b^* values are related to the chemical composition of celadon, phase structure, iron content, and valence state in the glaze, as well as the firing temperature and atmosphere [14,22]. Afterwards, a comprehensive study will be conducted on the glaze considering multiple coloring factors.

Table 1. Color value of celadon samples from the Lieshan Kiln.

Number	Dynasty	L*	a*	b*	Number	Dynasty	L*	a*	b*
BS1	Northern Song	38.65	0.45	13.27	JD1	Jin	43.63	1.24	20.10
BS2		55.09	0.02	16.10	JD2		44.31	0.13	19.89
BS3		27.27	1.07	6.01	JD3		44.10	−0.53	14.56
BS4		41.52	0.41	8.98	JD4		58.35	0.44	29.71
BS5		62.31	−0.28	16.67	JD5		54.58	2.48	27.79
BS6		36.01	1.61	13.99	JD6		45.33	1.01	20.14
BS7		35.96	0.96	11.45	JD7		51.44	2.05	28.71
BS8		22.00	0.98	7.37	JD8		35.71	1.37	10.11
BS9		24.57	1.46	6.23	JD9		61.88	1.07	32.68
				JD10	36.14		−0.05	7.01	
				JD11	45.23		1.98	18.25	

Selected specimens were analyzed for water absorption, apparent porosity, bulk density, and firing temperature, as detailed in Table 2. The results indicate that specimens from the Jin Dynasty exhibited higher firing temperatures compared to those from the Northern Song Dynasty, along with significantly lower water absorption rates and apparent porosity levels. This suggests that the specimens from the Jin Dynasty underwent a greater degree of sintering, leading to enhanced densification.

Table 2. The main physical properties of the bodies.

Number	Water Absorption/%	Apparent Porosity/%	Bulk Density/(g/cm ³)	Firing Temperature/°C
BS7	2.64	5.74	2.17	1131
BS9	3.62	8.06	2.23	1044
JD6	2.67	6.80	2.55	1180
JD11	1.81	4.11	2.28	1191

3.2. Chemical Composition Analysis of the Body

The chemical composition of the porcelain specimens' body is detailed in Table 3, including a comparative analysis of three types of raw materials sourced from the vicinity of the kiln site [5]. As indicated in Table 3, the Al₂O₃ content ranges from approximately 22 wt% to 30 wt%, with an average value of about 25.13 wt%, while SiO₂ content varies between approximately 63 wt% and 69 wt%, averaging around 66.69 wt%. As previously reported [2], the main chemical compositions of these specimens are highly similar to those of the white porcelain excavated from the Lieshan Kiln, with both exhibiting high aluminum and low silicon contents.

It is clear that Fe₂O₃ and TiO₂ are the coloring oxides in celadon. The average TiO₂ content in the body of Northern Song Dynasty celadon specimens is 0.54 wt%, while the average Fe₂O₃ content is 1.55 wt%. In contrast, Jin Dynasty celadon specimens exhibit an average TiO₂ content of 0.55 wt% and an average Fe₂O₃ content of 1.97 wt%. The increased levels of Fe₂O₃ and TiO₂ contribute to a predominantly grayish-white or dark-gray coloration of the specimens' bodies. Notably, Jin Dynasty specimens display a slightly higher Fe₂O₃ concentration compared to their Northern Song counterparts, which accounts for their marginally darker body color. According to the chemical and mineralogical composition of ceramic raw materials, sedimentary clays contain minimal amounts of TiO₂, whereas porcelain stones typically lack it altogether [23]. The TiO₂ content in these specimens suggests that the Lieshan Kiln utilized sedimentary clays as raw materials for body production. In Figure 1, it can be seen that elemental factors from both excavated ceramic raw materials and unearthed specimen bodies occupy similar regions, indicating

that the Lieshan Kiln’s celadon was produced using a single-ingredient formula derived from local sedimentary clays. Furthermore, analysis of microstructure in Figure 2 reveals significant quantities of kaolinite transformation products and quartz crystals within the body and trace amounts of feldspar, mica, and sphene. This proves that the Lieshan Kiln’s clay raw material is characterized by a mineralogical composition mainly rich in kaolinite with small amounts of illite [24].

Table 3. Chemical compositions of the Lieshan celadon bodies from different dynasties (wt%).

Number	Dynasty	SiO ₂	Al ₂ O ₃	Fe ₂ O ₃	TiO ₂	CaO	MgO	K ₂ O	Na ₂ O	MnO
BS1-b	Northern Song	67.34	25.51	1.56	0.53	1.08	0.97	1.48	0.53	0.02
BS2-b		67.53	22.62	1.34	0.43	1.72	0.66	1.24	0.47	0.02
BS3-b		67.78	24.22	1.72	0.5	1.49	0.9	1.75	0.64	0.1
BS4-b		67.45	23.52	2.18	0.44	2.26	1.12	1.68	0.36	0.01
BS5-b		64.81	27.6	1.67	0.51	1.14	0.91	1.74	0.62	0.01
BS6-b		69.19	23.75	1.65	0.6	1.1	0.62	1.87	0.22	0.02
BS7-b		67.17	25.77	0.9	0.56	1.52	0.62	1.79	0.68	0.01
BS8-b		62.86	30.29	1.17	0.7	1.77	0.6	1.35	0.28	0.02
BS9-b		68.85	24.34	1.74	0.6	0.89	0.77	1.77	0.04	0.02
JD1-b	Jin	65.87	26.14	1.92	0.6	1.19	0.91	1.92	0.45	0.02
JD2-b		67.65	25.44	1.76	0.58	0.78	0.81	1.95	0.03	0.02
JD3-b		68.11	23.9	1.84	0.59	2.11	0.49	1.56	0.39	0.03
JD4-b		65.63	26.61	1.86	0.54	1.15	0.96	1.74	0.51	0.03
JD5-b		66.61	23.4	2.89	0.64	1.72	1.03	1.85	0.85	0.02
JD6-b		62.81	26.73	2.03	0.49	3.11	1.18	2.02	0.63	0.02
JD7-b		65.91	24.88	1.82	0.43	1.73	0.88	2.76	0.6	0.03
JD8-b		67.63	23.14	1.85	0.47	2.79	0.75	1.98	0.75	0.02
JD9-b		66.02	25.01	2.08	0.56	2.03	0.91	1.26	1.13	0.04
JD10-b		67.83	24.28	1.95	0.49	1.14	0.92	1.8	0.59	0.03
JD11-b		66.78	25.48	1.72	0.61	1.14	0.79	1.83	0.66	0.03
LY-1	65.08	28.96	1.44	0.43	1.05	1.18	1.37	0.23	0.01	
LY-2	66.05	26.99	1.23	0.44	2.04	1.09	1.04	0.59	0.01	
LY-3	68.95	25.38	1.08	0.45	0.96	1.19	1.47	0.26	0.01	

Note: Fe oxides are denoted by Fe₂O₃, b for the body, and LY for raw material around the kiln site.

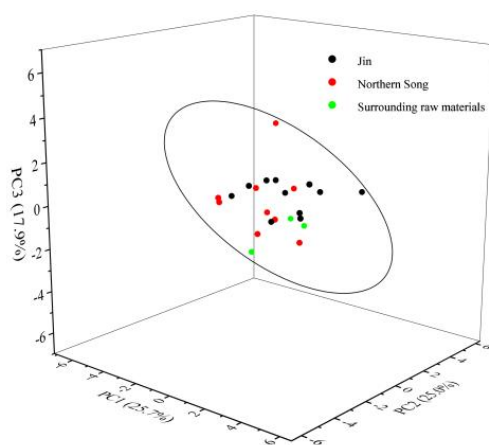


Figure 1. Principal component analysis diagram of raw materials around the kiln site and the body elements of the Lieshan Kiln samples.

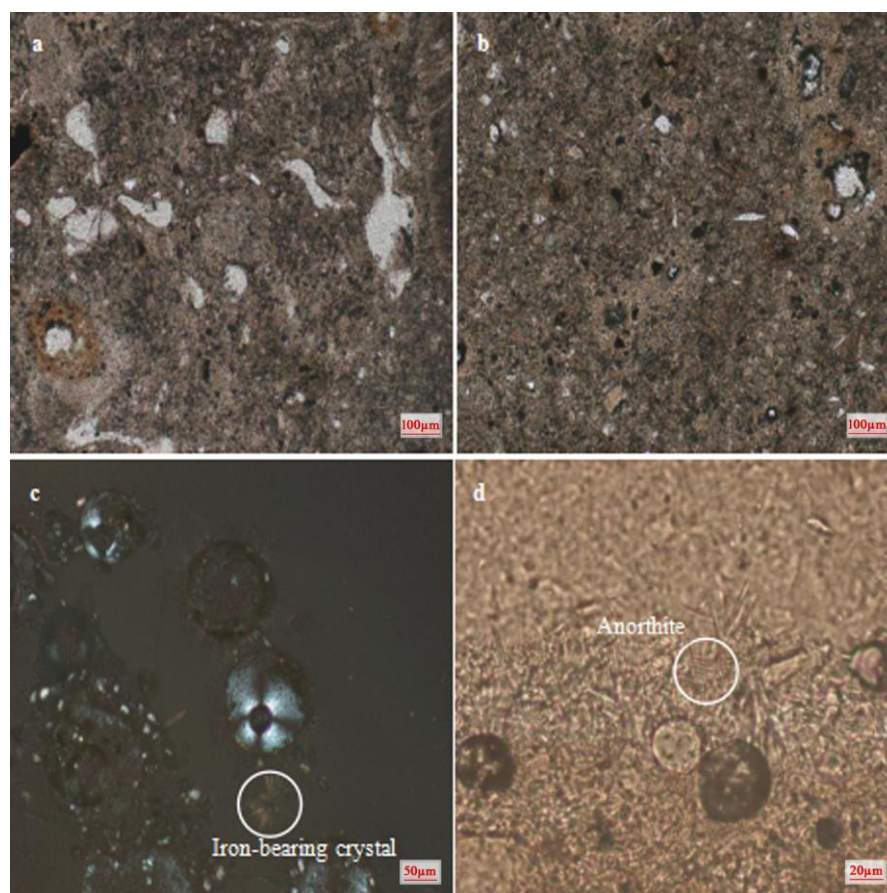


Figure 2. Polarized microstructure diagram of celadon samples of Lieshan Kiln: (a) sample BS7 body; (b) sample JD10 body; (c,d) sample JD10 glaze in cross-section.

Furthermore, Figure 1 illustrates that the elemental composition of the ceramic body from the Northern Song Dynasty displays greater variability, suggesting that there were more advanced the washing and refining processes for body materials during the Jin Dynasty compared to Northern Song Dynasty. Analysis of the characteristics of these bodies reveals that specimens from the Northern Song Dynasty contain a significant number of irregularly sized black and white particles, with glaze surfaces often exhibiting protruding coarse sand grains, resulting in a noticeably coarser texture compared to Jin Dynasty specimens. The optical microstructure diagrams in Figure 2a,b demonstrate that specimen JD-10 contains fewer and smaller coarse particle impurities within its body relative to specimen BS-7. This further implies that processing techniques during the Jin Dynasty were more refined, effectively eliminating some coarse-grained quartz and other impurities. Overall, there was a more refined selection of body materials and processing methods during the Jin Dynasty.

As indicated in the chemical composition of fluxing agents in the celadon body, the content of RO and R₂O oxides in specimens from both periods is relatively low. The average total content of RO + R₂O in Northern Song Dynasty specimens is 4.29 wt%, while the content increases to 5.07 wt% in Jin Dynasty specimens. Compared with the Northern Song specimens, the Jin Dynasty specimens have a slightly higher content of molten oxides, which is more likely to promote body sintering under the same firing regime. Coupled with the increased firing temperatures of the Jin Dynasty in Table 2, this resulted in a higher degree of sintering and greater density in the Jin Dynasty specimens. This phenomenon is consistent with their external appearance. During the Northern Song Dynasty, the Lieshan Kiln was already renowned for its prosperous kiln industry and extensive trade,

showing the exquisite porcelain-making techniques of the time. However, with the demise of the Northern Song Dynasty and the signing of the “Shaoxing Peace Treaty”, the kiln site entered a recovery period during the Jin Dynasty. Although the quantity decreased, the kiln industry did not come to a halt. As a porcelain kiln site along the Tongji Canal, the porcelain-making techniques of this period inherited the firing technology from the Northern Song Dynasty and continuously improved under the influence of the high standards of the Southern Song Dynasty’s porcelain industry. This caused a noticeable enhancement in the quality of the Lieshan Kiln’s ceramics during the same period and thus affirmed ongoing development and innovation within ceramic techniques amidst historical transitions.

3.3. Chemical Composition Analysis of the Glaze

The chemical composition of the glaze on the celadon specimens is detailed in Table 4. The average total content of RO in Northern Song Dynasty specimens is 14.53 wt%, while that of R₂O averages 4.01 wt%. In contrast, for Jin Dynasty specimens, the average total content of RO reaches 13.41 wt%, and R₂O averages 3.62 wt%. Based on the classification of ancient Chinese Ca-series glazes according to their glaze coefficient b value, calcium glazes can be categorized into three types: calcium glaze ($b \geq 0.76$), calcium-alkali glaze ($0.76 > b \geq 0.5$), and alkali-calcium glaze ($b < 0.50$). The coefficient b in the Seger formula reflects the ratio of these two groups of oxides. The form of the formula is $aR_2O \cdot bRO \cdot cR_2O_3 \cdot dRO_2$, where R₂O and RO represent alkali oxides and alkaline earth oxides, respectively, R₂O₃ and RO₂ represent trivalent and tetravalent oxides, respectively, and the coefficients a, b, c, and d correspond to the molar quantities of each type of oxide when (R₂O + RO) equals 1 [25,26]. Figure 3 demonstrates that the b value of celadon glaze from both Northern Song and Jin Dynasties exceeds 0.76, with a few exceptions. This indicates that they belong to the category of high-calcium glazes.

Table 4. Chemical compositions of the Lieshan celadon glazes from different dynasties (wt%).

Number	Dynasty	SiO ₂	Al ₂ O ₃	Fe ₂ O ₃	TiO ₂	CaO	MgO	KO ₂	NaO ₂	MnO	P ₂ O ₅	SiO ₂ /Al ₂ O ₃
BS1-g	Northern Song	62.34	11.24	3.17	0.27	16.63	2.72	2.36	0.26	0.08	0.26	9.43
BS2-g		61.15	16.06	1.73	0.31	13.20	1.91	4.18	0.45	0.07	0.21	6.47
BS3-g		69.7	11.91	3.13	0.29	8.37	1.43	3.88	0.28	0.06	0.13	9.95
BS4-g		58.17	9.94	4.28	0.41	21.69	2.35	1.72	0.44	0.10	0.37	9.95
BS5-g		57.94	15.54	3.18	0.30	13.13	3.17	5.33	0.40	0.05	0.37	6.34
BS6-g		64.82	14.18	3.20	0.28	10.10	1.98	3.65	0.79	0.07	0.27	7.77
BS7-g		69.22	11.92	2.60	0.32	9.37	1.67	2.83	1.06	0.05	0.15	9.87
BS8-g		66.08	10.5	2.91	0.27	13.56	1.96	3.69	0.03	0.07	0.25	10.70
BS9-g		75.59	8.40	2.43	0.27	6.66	0.89	3.10	1.66	0.06	0.07	15.30
JD1-g	Jin	63.89	12.69	2.39	0.34	11.29	2.58	5.06	0.76	0.07	0.23	8.56
JD2-g		66.11	11.5	2.49	0.32	9.38	2.03	5.54	1.63	0.05	0.15	9.77
JD3-g		65.65	12.62	3.06	0.31	10.73	3.08	3.28	0.27	0.07	0.44	8.84
JD4-g		66.68	11.97	2.80	0.32	12.37	2.02	2.37	0.47	0.08	0.21	9.47
JD5-g		64.96	11.56	3.67	0.34	14.10	2.07	1.93	0.38	0.08	0.25	9.55
JD6-g		72.33	11.35	3.38	0.43	6.27	1.74	2.68	0.82	0.05	0.16	10.83
JD7-g		66.29	11.71	2.9	0.28	13.09	2.05	2.21	0.46	0.08	0.25	9.62
JD8-g		65.38	11.48	2.79	0.33	14.17	2.61	1.85	0.41	0.09	0.38	9.68
JD9-g		67	11.72	2.23	0.32	14.13	1.8	1.77	0.03	0.08	0.27	9.72
JD10-g		72.89	9.28	2.18	0.31	8.81	1.71	3.06	0.76	0.09	0.21	13.35
JD11-g		71.59	9.51	2.06	0.27	9.96	1.5	3.37	0.74	0.09	0.13	12.80

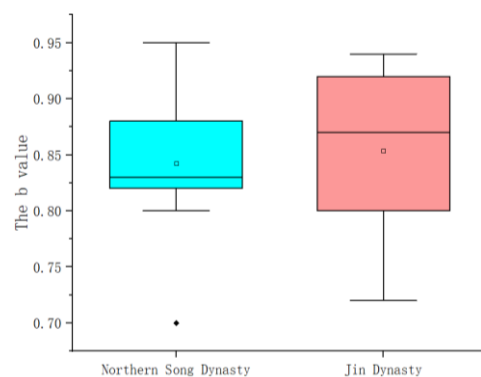


Figure 3. The coefficient b value of the celadon samples.

The glaze of the celadon specimens contains an average of approximately 0.24 wt% P_2O_5 , as well as a minor quantity of MnO. According to archaeological findings at Guantai Kiln, the utilization and preparation of glaze ash can be traced back to at least the Northern Song Dynasty during Emperor Huizong's reign [27]. Regarding plant ash, glaze ash, and clay-based porcelain raw materials, it is established that plant ash typically contains a higher content of P_2O_5 and MnO. Glaze ash exhibits high levels of CaO while containing lower amounts of P_2O_5 and MnO, whereas clay-based materials generally contain less than 0.02 wt% MnO, with P_2O_5 present only as a trace element. The presence of P_2O_5 in the celadon glaze without high amounts indicated that plant ash-like materials were added to the glaze materials at the Lieshan Kiln. Comparative analysis of the development of porcelain glazes and glaze ashes in Jingdezhen during the Tang, Five Dynasties, and Song Dynasties indicates that the Lieshan Kiln employed primary-stage glaze ash (calcined and washed limestone) [28]. Furthermore, the concentrations of iron and titanium within the glaze implied that alongside plant ash for glazing purposes, a type characterized as high-iron low-titanium sedimentary clay was also utilized. As illustrated in Figure 4, it is evident that Fe_2O_3 content in the glaze of specimen exceeds that found within its body, while TiO_2 content is significantly lower than that present in the body. This difference suggests a different source of raw materials for the glass and body manufacturing processes.

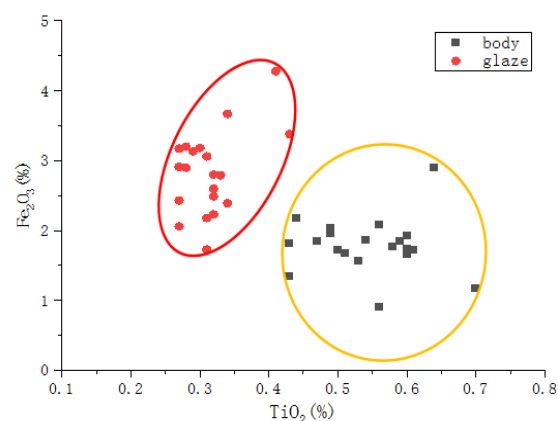


Figure 4. Scatter plot of TiO_2 and Fe_2O_3 in the bodies and glazes of the samples.

3.4. Chemical Valence Analysis of Fe Ions

The celadon glaze exhibits an average Fe_2O_3 content of approximately 2.83 wt%. Utilizing X-ray photoelectron spectroscopy (XPS) and the Avantage software 6.8.1 for peak fitting, the Fe^{2+}/Fe^{3+} ratio in the glazes of specimens BS-8 and JD-11 was analyzed, with the results shown in Figure 5. The fitted peak areas revealed that the Fe^{2+}/Fe^{3+} ratios were 35.37/64.63 and 43.15/56.85, respectively, indicating a higher concentration of

Fe^{3+} compared to Fe^{2+} . In the reducing atmosphere, some of the Fe^{3+} present in the glaze was partially reduced to Fe^{2+} . This, together with the observation that the glaze colors range from gray-green to yellow-green and even soy sauce-like green shades, comprehensively illustrates that the firing atmosphere of the Northern Song and Jin dynasties was a weakly reducing atmosphere.

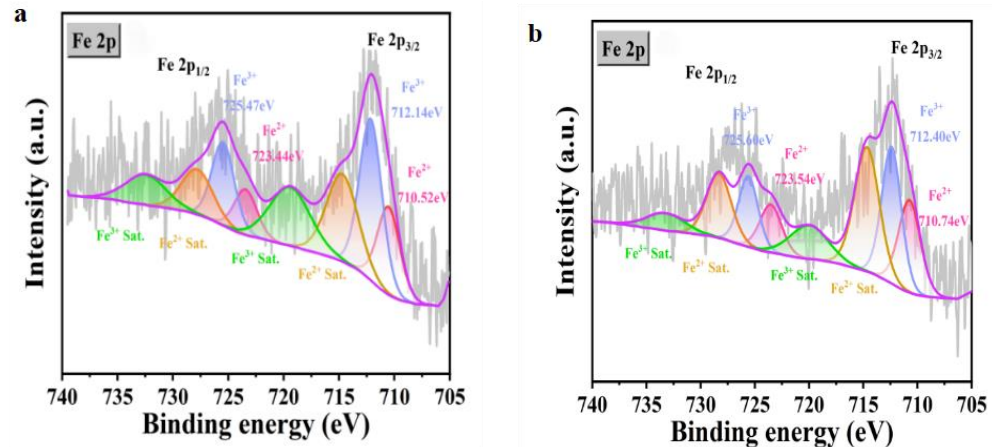


Figure 5. XPS fitting map of celadon samples from the Lieshan Kiln: (a) sample BS8; (b) sample JD11.

As a 3D element, iron has an electron configuration of $[\text{Ar}]3d^64s^2$. Its electrons can be easily transformed to form divalent iron (Fe^{2+}) with the configuration $[\text{Ar}]3d^64s^0$ and trivalent Fe ions (Fe^{3+}) with the configuration $[\text{Ar}]3d^54s^0$. In the glaze melt, Fe ions exist in two structural states: octahedral 6-coordinate $[\text{FeO}_6]$ and tetrahedral 4-coordinate $[\text{FeO}_4]$. These two coordination states allow for different colorations and properties in the glaze, as the electronic transitions between these states can influence the glaze's optical and magnetic properties. As the concentration of Fe_2O_3 increases in the glaze melt, the $[\text{FeO}_4]$ complex transforms into the $[\text{FeO}_6]$ complex, and this change in coordination number results in alterations to the crystal field energy, significantly affecting light absorption behavior and coloration within the glaze [29]. Due to the higher field strength of Fe^{3+} compared to Si^{4+} , Fe^{3+} can be integrated into the network structure of the glaze melt, existing in a tetrahedral $[\text{FeO}_4]$ form. This further facilitates crystal melting and contributes to the formation of a non-crystalline structure. This enhances immiscibility within the glaze system, effectively promoting a phase-separated structure [30]. Furthermore, due to the smaller radius but larger charge number of Fe^{3+} compared to that of Fe^{2+} , its potential energy Z/r exceeds that of Fe^{2+} , resulting in a smaller potential difference $\Delta Z/r$ when compared with Si^{4+} oxides. This makes Fe^{3+} more susceptible to phase separation. During the Jin Dynasty, specimens were fired at temperatures exceeding those during the Northern Song Dynasty. In this firing process, high temperatures favorably promote the decomposition of Fe_2O_3 into FeO and O_2 , thereby increasing the ratio of $\text{Fe}^{2+}/\text{Fe}^{3+}$ in glazes from Jin Dynasty specimens. The increase in melting temperature shifts the equilibrium towards greater formations of Fe^{2+} . In specimen BS8, content levels for total iron oxide are greater than those found in specimen JD11. This increase contributes to shifting the equilibrium towards additional formations of Fe^{3+} , consistent with XPS test results. Meanwhile, the field strength of P^{5+} exceeds that of Si^{4+} . The pentavalent phosphorus exhibits a greater capacity to compete for free oxygen than Si^{4+} , thereby enhancing immiscibility within the glaze system [31]. Additionally, trace amounts of P_2O_5 in the glaze further facilitate phase separation.

3.5. Analysis of the Microstructure and the Coloring Mechanism

As shown in Figure 6, the celadon glaze exhibits isolated spherical droplet phase separation structures. In the glassy phase, decomposition within the $\text{SiO}_2\text{-Al}_2\text{O}_3\text{-CaO}$

metastable region tends to facilitate the formation of these isolated spherical droplets. The phase-separated particles observed in the celadon glaze range from 10 to 20 nm in size (Figure 6). These particles are sufficiently small to avoid Rayleigh or Mie scattering, allowing light to pass directly through the glaze layer. Therefore, the glaze color is mainly influenced by the chemical coloring produced by iron ions. This suggests that the celadon glaze from the Lieshan Kiln is a unique transparent glaze characterized by a phase-separated structure.

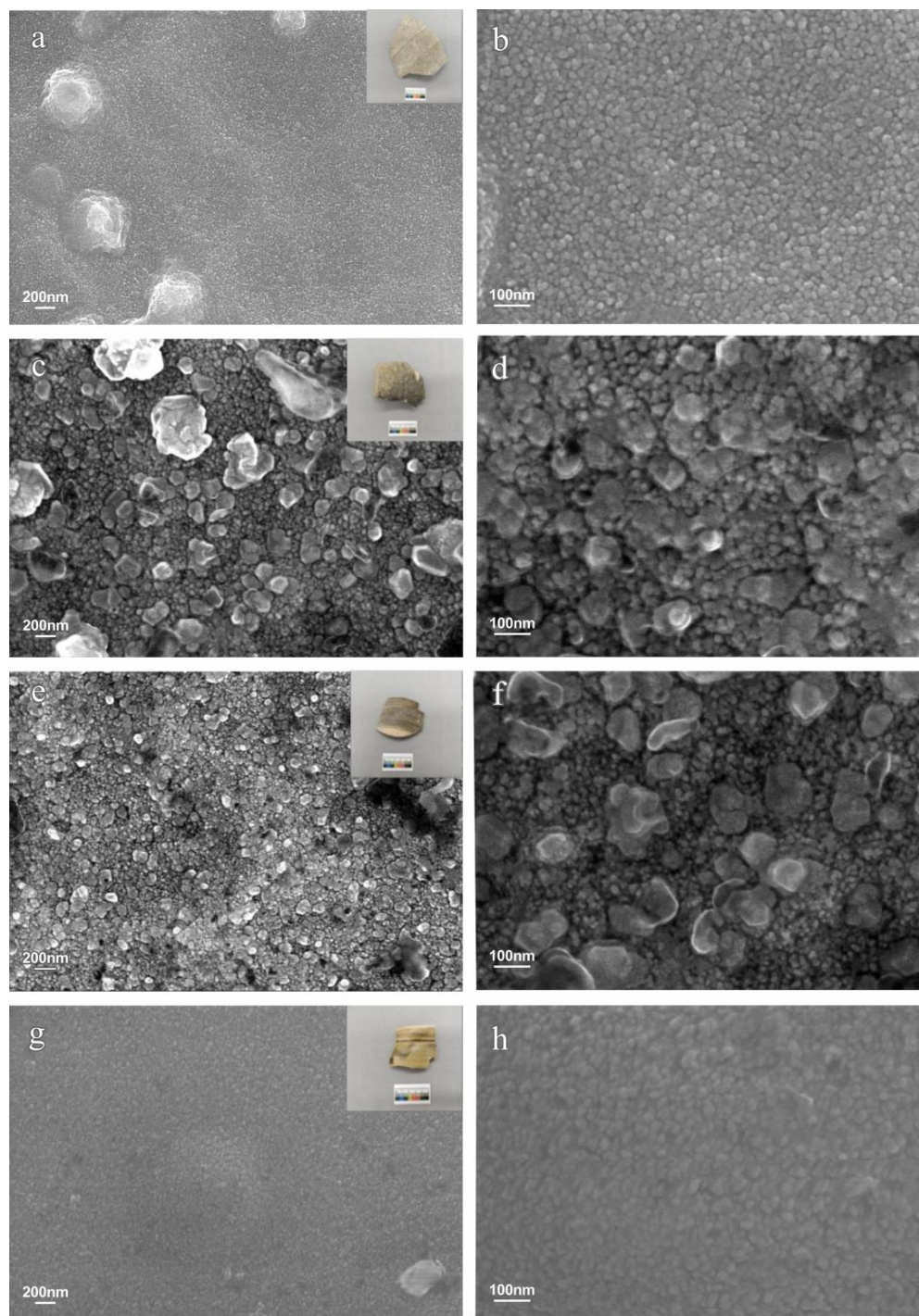


Figure 6. Scanning electron microscope images of celadon samples: (a,b) sample BS2; (c,d) sample BS4; (e,f) sample JD3; (g,h) sample JD4.

The glaze composition of the celadon specimens is characterized by a SiO_2 content of 58–75 wt%, with an average of about 66.39 wt%, and an Al_2O_3 content of 8–17 wt%, averaging approximately 11.75 wt%. As illustrated in Table 4, celadons from both the Northern Song and Jin Dynasties typically exhibit high $\text{SiO}_2/\text{Al}_2\text{O}_3$ molar ratios, with mean values of approximately 9.53 and 10.2, respectively. This increased molar ratio of SiO_2 to Al_2O_3 in the glaze facilitates the extensive formation of phase-separated droplets [32]. Figure 2d illustrates the calcium feldspar crystals within the intermediate layer between the glaze and body, suggesting that a local reduction in Al_2O_3 in the glaze occurs during formation, which subsequently elevates the $\text{SiO}_2/\text{Al}_2\text{O}_3$ ratio and enhances liquid phase separation. Notably, even specimens BS2 and JD3, exhibiting $\text{SiO}_2/\text{Al}_2\text{O}_3$ molar ratios of 6.47 and 8.84, respectively, demonstrate phase-separated structures, as shown in Figure 6a,b,e,f. This observation implies that although the formation of phase separation structures is influenced by the $\text{SiO}_2/\text{Al}_2\text{O}_3$ molar ratio, it is also significantly affected by other chemical components such as Fe_2O_3 . Higher concentrations further promote phase separation processes, indicating that phase separation in Lieshan Kiln celadon stems from a complex interplay among various chemical compositions.

Fe ions in celadon glaze function as coloring agents and facilitate the formation of phase separation. The combined effects of Fe^{3+} and Fe^{2+} account for the coloration observed in the Lieshan Kiln celadon glaze. The celadon glaze specimens exhibit a high molar ratio of $\text{SiO}_2/\text{Al}_2\text{O}_3$, positioning them within the phase-separated region. Additionally, elevated concentrations of Fe_2O_3 and trace amounts of P_2O_5 further promote phase separation. In comparison to the Lieshan Kiln, despite the lower Fe_2O_3 content of the Yue Kiln (approximately 2 wt%), its lower $\text{SiO}_2/\text{Al}_2\text{O}_3$ molar ratio precludes the development of a phase-separated glaze. The Yaozhou Kiln, with an average $\text{SiO}_2/\text{Al}_2\text{O}_3$ molar ratio of approximately 8.9, slightly lower than that of the Lieshan Kiln celadon glazes, also fails to exhibit phase separation due to its higher firing temperature (around 1300 °C) after the Five Dynasties, which leads to the destruction of phase separation structures within the glaze. Thus, it is classified as a non-phase-separated transparent celadon glaze [33]. This underscores that the Lieshan Kiln celadon glaze represents a distinct type of transparent glaze characterized by its unique phase-separated structures.

4. Conclusions

Lieshan Kiln celadon is a distinct category of transparent glaze distinguished by phase separation structures. It has the following characteristics:

(1) The celadon specimens from the Northern Song and Jin Dynasties were crafted from local raw materials using a single-ingredient formula based on sedimentary clays. The preparation of body materials during the Jin Dynasty was more refined compared to those during the Northern Song Dynasty. In terms of the physical properties, the bodies from Jin Dynasty exhibit greater density and are fired at slightly higher temperature than those from the Northern Song Dynasty.

(2) The glaze of celadon in the Lieshan Kiln belongs to a high-calcium glaze category. The glaze raw materials consist of glaze ash (calcined and elutriated limestone) along with high-Fe, low-Ti sedimentary clays distinct from those used in body materials. The firing atmosphere was weakly reduced, resulting in deeper green glaze coloration with increased concentrations of Fe_2O_3 and TiO_2 .

(3) Celadon glaze exhibits a high $\text{SiO}_2/\text{Al}_2\text{O}_3$ molar ratio that falls within the phase separation region. Increased concentrations of Fe_2O_3 and trace amounts of P_2O_5 as a phase separation agent facilitate the formation of phase separation structure within the glaze matrix.

(4) The coloration observed in celadon glaze arises from the combined effects of Fe^{3+} and Fe^{2+} ions. When phase-separated particles are sufficiently small to avoid Rayleigh or Mie scattering, glaze color is mainly determined by chemical coloration produced by Fe ions.

Supplementary Materials: The following supporting information can be downloaded at: <https://www.mdpi.com/article/10.3390/cryst15010095/s1>, Table S1: Detailed characteristic information of Lieshan Kiln samples.

Author Contributions: Conceptualization, J.W.; methodology, Q.L. and J.L.; software, J.W. and C.G.; validation, C.C. and T.F.; formal analysis, T.F.; investigation, Q.L. and C.C.; resources, C.C. and C.G.; data curation, J.W., T.F., and C.G.; writing—original draft, Q.L., J.W. and J.L.; writing—review and editing, Q.L. and J.L.; supervision, C.C. and J.L.; project administration, T.F. and C.G.; funding acquisition, Q.L. and J.L. All authors have read and agreed to the published version of the manuscript.

Funding: This research was financially supported by the National Natural Science Foundation of China (52462003), the Social Science Fund of Jiangxi Province (23YS15), the Jiangxi Ceramic Heritage Conservation and Imperial Kiln Research Collaborative Innovation Center Project (JXYY2304), and the Graduate Student Innovation Fund of Jingdezhen Ceramic University (JYC202421).

Data Availability Statement: All data are included in text.

Conflicts of Interest: The authors declare no conflicts of interest.

References

1. Institute of Cultural Relics and Archaeology of Anhui; Huaibei Municipal Bureau of Cultural Relics; Huaibei Museum. *The Lieshan Kiln Site in Huaibei (All Two Volumes)*; Cultural Relics Press: Beijing, China, 2022. (In Chinese)
2. Ma, Y.Y.; Chen, C.; Li, H.; Kang, B.Q. Scientific analysis of white porcelains unearthed from Lieshan Kiln, Anhui Province. *Chin. Ceram.* **2020**, *41*, 729–735. (In Chinese with English abstract) [[CrossRef](#)]
3. Sang, Y.X.; Zheng, N.Z.; Wu, J.M.; Wang, L. Study on porcelain production process based on modern test and analysis method in Lieshan Kiln. *Chin. Ceram.* **2021**, *2*, 61–69. (In Chinese with English abstract) [[CrossRef](#)]
4. Sang, Y.X.; Zheng, N.Z.; Wu, J.M. Influence of Northern Kilns on body and glaze composition of Lieshan Kiln porcelain in Huaibei. *Chin. Ceram.* **2021**, *6*, 62–68. (In Chinese with English abstract) [[CrossRef](#)]
5. Feng, X.M. *Illustrated Dictionary of Ancient Chinese Ceramics*; Cultural Relics Press: Beijing, China, 1998; pp. 52–53. (In Chinese)
6. Lv, C.L. Briefly discuss the body glaze characteristics of the Southern Song official kiln celadon. *Collect. J.* **2017**, *10*, 45–47. (In Chinese)
7. *Bureau of Light Industry in Zhejiang Province, Study on the Longquan Celadon*; Press of cultural Relics: Beijing, China, 1989; pp. 1–2.
8. Zhou, S.H. Further study on the celadon glaze in longquan kiln from the Songdynasty. *Chin. Ceram.* **1999**, *4*, 36–39. [[CrossRef](#)]
9. Shu, Y. Research on Celadon and Zen From the Perspective of Contemporary Aesthetics. *J. Ceram.* **2019**, *40*, 866–868. [[CrossRef](#)]
10. Wang, X.M. Analysis of azure blue porcelain the from the Yaozhou Kiln. *Archaeol. Cult. Relics* **2019**, *15*, 31–38.
11. Li, Y.; Zhang, B.; Cheng, H.; Zheng, J. Revealing the coloration mechanism in the earliest Chinese celadon glaze. *J. Eur. Ceram. Soc.* **2019**, *39*, 1675–1682. [[CrossRef](#)]
12. Zhang, B.; Gao, X.L. PIXE and Mössbauer spectroscopy analysis of Yue celadon unearthed from Hehuaxin kiln site, China. *Nucl. Instrum. Meth. B* **2024**, *551*, 165350. [[CrossRef](#)]
13. Wang, Y.; Yu, S.; Chu, J.; Chen, D.; Chen, J. Study on the copper and iron coexisted coloring glaze and the mechanism of the fambe. *J. Eur. Ceram. Soc.* **2018**, *38*, 3681–3688. [[CrossRef](#)]
14. Shi, P.; Wang, F.; Zhu, J.; Zhang, B.; Zhao, T.; Wang, Y.; Qin, Y. Study on the Fivedynasty sky-green glaze from Yaozhou kiln and its coloring mechanism. *Ceram. Int.* **2017**, *43*, 2943–2949. [[CrossRef](#)]
15. Xiao, Y.F.; He, M.H.; Zhang, S.D.; Hang, W. Mass spectrometric methods for colorativemechanism analysis of Yaozhou porcelain glaze. *Spectrosc. Spectr. Anal.* **2015**, *35*, 2444–2449.
16. Zhang, B.; Gao, Z.Y. NAA and Mössbauer study on the colorative mechanism of Yaozhou celadon in ancient China. *Hyperfine Interact.* **2002**, *142*, 593–599.
17. Wang, T.; Chen, P.; Wang, M.; Sang, Z.; Zhang, P.; Wang, F.; Sciau, P. Micro-structural study of Yaozhou celadons (Tang to Yuan Dynasty): Probing crystalline and glassy phases. *J. Eur. Ceram. Soc.* **2020**, *40*, 4676–4683. [[CrossRef](#)]
18. Sang, Z.; Fu, X.Y.; Wu, M.J.; Shen, Z.Z.; Shen, S.R.; Yuan, X.J. Study on the coloring mechanism of Longquan light greenish-blue celadon glaze from the Southern Song and Yuan Dynasties. *Ceram. Int.* **2023**, *49*, 13249–13257. [[CrossRef](#)]

19. Zhang, B.; Zhang, M.; Li, Y.; Cheng, H.; Zheng, J. PIXE study on recovery of making-technology of Chinese Longquan celadon made in the Southern Song Dynasty (1127-1279 CE). *Ceram. Int.* **2019**, *45*, 3081–3087. [[CrossRef](#)]
20. Chen, F.; Wu, L.H.; Zhao, E.L. *Introduction to Colored Glass*; Chemical Industry Press: Beijing, China, 2009; pp. 84–92. (In Chinese)
21. Wu, J.; Wu, J.; Li, Q.; Li, J.; Luo, H.; Deng, Z. *Scientific and Technological Achievements in Ancient Chinese Ceramics Pottery and Porcelain*; Shanghai Scientific Technical Publishers: Shanghai, China, 1985; pp. 239–256. (In Chinese)
22. Sang, Z.; Wang, F.; Duan, X.; Mu, T.; Ren, Z.; Wei, X.; Yuan, X.; Jiao, Y. Analysis of the celadon characteristics of the Yaozhou kiln. *Ceram. Int.* **2019**, *45*, 22215–22225. [[CrossRef](#)]
23. Ma, T.C. *Ceramics Technology*; China Light Industry Press: Beijing, China, 2013; pp. 29–31. (In Chinese)
24. Chen, Z.T.; Tian, B.L. Clay minerals in clay ores at LieShan. Huaibei. Anhui Province. *Acta. Miner. Sci.* **1981**, *4*, 254–256. [[CrossRef](#)]
25. Luo, H.J.; Li, J.Z.; Gao, L.M. Classification criteria of calcium glaze types in Chinese ancient porcelain and its application in enamel research. *Bull. Chin. Ceram. Soc.* **1995**, *2*, 50–53.
26. Li, J.; Yang, Y.; Zou, D.; Wu, L.; Wu, Q.; Lin, Z.; Li, Q. Recognition of Yuan blue and white porcelain produced in Jingdezhen based on graph anomaly detection combining portable X-ray fluorescence spectrometry. *Herit. Sci.* **2024**, *12*, 79. [[CrossRef](#)]
27. Qin, D.S. A new study of glaze ash. *Archaeology.* **2001**, *10*, 78–82.
28. Li, Q.J.; Zhang, M.L.; Xiong, L.; Ji, Y.; Wu, J. Development and Evolution of Jingdezhen Lime-ash. *Chin. Ceram.* **2020**, *1*, 115–120. [[CrossRef](#)]
29. Huang, X.C.; Zhan, H.Q.; Liu, Q.; Song, Y.; He, S.; Li, F.; Wang, C.; Xie, Z. Correlation between glaze color and crystallization process of Fe₂O₃ in glaze melt. *J. Chin. Ceram. Soc.* **2022**, *9*, 2448–2454.
30. Hu, Z.Q. *Fundamentals of Inorganic Materials Science*; Chemical Industry Press: Beijing, China, 2004; pp. 18–34. (In Chinese)
31. Yang, C.A. Research on Separative-Phase Glaze and Its Structural Color. Ph.D. Thesis, Shaanxi University of Science and Technology, Xi'an, China, 2016. (In Chinese)
32. Sun, H.W.; Chen, X.Q.; Gao, L.M. Immiscibility and crystallization of 0.20R₂O-0.25CaO-0.55ZnO-Al₂O₃-SiO₂ system. *Chin. Ceram.* **2000**, *4*, 13–17. [[CrossRef](#)]
33. Liu, P.; Wang, F.; Luo, H.; Zhu, J.; Shi, P.; Hao, Y.; Feng, B. Comparative study on celadon glazes of Five Dynasty Yaozhou Kiln. Northern Song Dynasty Ru Kiln and Southern Song Dynasty Guan Kiln. *J. Chin. Ceram. Soc.* **2020**, *48*, 1935–1943.

Disclaimer/Publisher's Note: The statements, opinions and data contained in all publications are solely those of the individual author(s) and contributor(s) and not of MDPI and/or the editor(s). MDPI and/or the editor(s) disclaim responsibility for any injury to people or property resulting from any ideas, methods, instructions or products referred to in the content.